The electromagnetic properties of amorphous and nanocrystalline powdered Fe-Si-B-Cu-Nb alloy at microwaves

Roman Kubacki, Rafał Przesmycki, Marian Wnuk,
Member, IEEE

Faculty of Electronics, Military University of Technology
Warsaw, Poland
romankubacki@onet.pl

Jarosław Ferenc

Faculty of Materials Science and Engineering, Warsaw University of Technology
Warsaw, Poland
jferenc@inmat.pw.edu.pl

Abstract—**The electric and magnetic properties of the magnetically soft Fe-Si-B-Nb-Cu alloy (Finemet), as a candidate on the absorber at microwaves, have been studied in the frequency range from 0.2 to 10 GHz. Measurements were achieved with the use of the coaxial line technique, where the scattering parameters at broadband frequency range were determined. In this method, using the signal flow graph representation, a method of measuring of the powders inserted in between two plastic walls has been discussed. Based on this attempt, values of relative permittivity (ε', ε") and permeability (μ', μ") of the powdered amorphous and nanocrystalline Finemet were shown for four groups of powders with different particle sizes. The measured data refers to pure pulverized Finemet without insulating resin or wax. The obtained results show that the powdered nanocrystalline Finemet containing particles below 25 μm in diameter can have good shielding / absorbing properties (EMC).**

Keywords- NanoEMC, Nanocrystalline, Amorphous, Finemet, Permittivity and permeability measurements, Microwave absorbers.

I. INTRODUCTION

Nowadays, technology offers a variety of nonconventional materials with unique mechanical and physical properties. At higher frequencies, due to miniaturizing of elements and construction simplifications, the improved magnetic properties of the materials are needed for electronic equipment taking into account the EMC requirements. In fact, the possible range of magnetic material applications grow with an improvement of the magnetic properties. Among candidates for new absorbers at microwaves, the soft magnetic materials present a kind of interesting materials. Soft magnetic materials are characterized by low coercivity and high permeability. Metallic glasses based on iron and/or cobalt can be very attractive soft magnetic materials fulfilling such requirement. The nanocrystalline alloys (FeSiBCuNb) are closely related to the amorphous soft magnetic materials. The precursor amorphous FeSiB alloy, containing small additions of Nb and Cu, is rapidly quenched into 20μm thick ribbons ("Finemet" – HITACHI, "Vitroperm" – VACUUMSCH MELZE, "NanoPhY" – IMPHY). Amorphous metallic glasses are used as precursors to produce nanocrystalline alloys. The material is annealed at temperature around 550°C to induce optimum crystallization, allowing it to obtain the mean grain size of 10-15 nm. Nanocrystalline alloys are developed to obtain great permeability. Finemet ($Fe_{73.5}Si_{13.5}B_9Nb_3Cu_1$), elaborated by Yoshizawa et al. [1], was the first alloy of this type. The magnetic properties of Finemet were presented in [2, 3, 4, 5, 6], however, this data was investigated in low frequency range, below 10 MHz demonstrating excellent magnetic properties. It turned out that the relative permeability is ten times higher than these of MnZn or NiZn ferrites [1, 3].

For the nanocrystalline Finemet, the low coercivity and high permeability were obtained with small grain sizes less than the ferromagnetic exchange length, which is in opposite to classical theory [2, 4, 7]. Herzer [2, 7] showed that initial permeability can be significantly enhanced when the grain sizes are smaller than 20 nm in diameter. The electric and magnetic properties of nanocrystalline Finemet in the frequency range from 0,2 to 10 GHz was presented in our previous study [11]. In this work the permittivity and permeability of amorphous Finemet were presented and compared to the nanocrystalline phase. Measurements of powdered Finemet with optimal 14 nm mean grain diameter were presented for four groups of powders to investigate the relationship of electric and magnetic properties as the function of particle size. Measurements were taken from pure powders, without resin, wax, or other glues, i.e. without insulating substances affecting the internal properties. The obtained data can be useful to design the effective absorbers at microwaves.

II. STRUCTURE OF THE MATERIAL

Finemet ribbons were obtained by melt spinning into a single amorphous phase. The quenched ribbons were fully amorphous, which was confirmed by means of X-ray diffractometry. Amorphous Finemet powder was prepared by ball milling of the amorphous ribbons. The obtained powder was divided into two parts: the first one was subjected to stress relieving (annealing at 400°C for 30 minutes) and the second part was crystallized at 540°C for 60 minutes to receive the nanocrystalline structure. The final structure was composed of ultrafine α-Fe(Si), occupying about 70% of the alloy's

978-1-4673-0717-8/12/$31.00 ©2012 IEEE

volume, embedded in the residual amorphous matrix. The grain size was controlled by annealing condition, resulting in extremely small grain sizes. The amorphous and nanocrystalline powders were used to compare their electromagnetic properties. Figure 1 shows the XRD patterns of the amorphous and nanocrystalline powder structures.

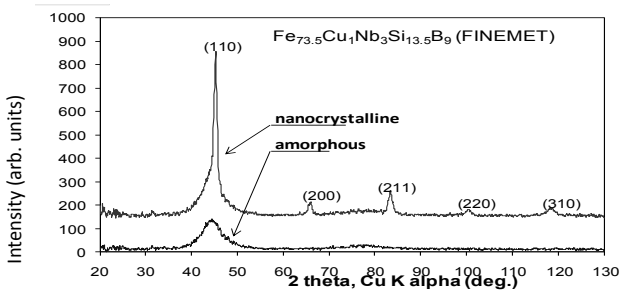

Fig. 1. X-ray diffraction patterns of amorphous and nanocrystalline Finemet.

Fig. 1 shows that the powder obtained from melt-spun ribbon has a fully amorphous structure. The nanocrystalline material was obtained by annealing at 540 for 1 h. The average grain size calculated from the α-Fe(Si) peak was assessed to be around 14 nm.

III. Coaxial Line Method of Permittivity and Permeability Measurement

The permittivity and permeability measurements of solid and non-solid materials are commonly performed using coaxial fixtures. At microwaves, the coaxial line technique is especially recommended for broadband frequency measurements. The method of measuring of ε and μ, based on determining the scattering parameters (S_{ik}) of the measured sample is the most popular [6, 8, 9, 10]. In such a case, the measured material completely fills the cross section of the holder. This configuration guarantees that the only TEM mode propagates.

For the measurements of powdered materials in coaxial lines, two additional walls have to be used. In such a case, the measured sample will be a composite material, consisting of powdered material and two walls as shown in Fig. 2. In fact, the walls can be made of any dielectric material, because the properties of walls are determined in additional measurements.

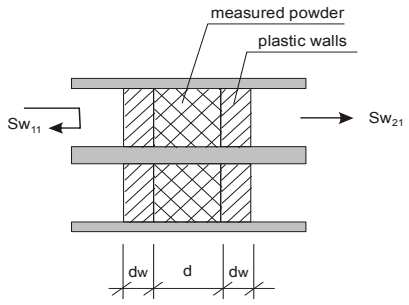

Fig. 2. The sketch of coaxial line with a sample of powdered material under test between 2 walls.

The set-up presented in Fig.2 consists of 3 line-elements, eg. 2 plastic walls and a sample of measured powder. In the designed technique, there is a requirement that both walls have the same length to fulfill the symmetrical properties of the entire composite. Such a network can be described by transmission matrices and the resultant transmission matrix of whole network can be written as follows, as it was developed in our previous work [11]:

$$\mathbf{Tw} = \mathbf{TE\ TS\ TE} \tag{1}$$

where: **Tw** – transmission matrix of whole network,
TE – transmission matrix describing wall,
TS – transmission matrix of a powder-sample.

De-embedding technique can be used to solve the transmission matrix **TS** and afterwards the scattering coefficients **S** can be calculated. De-embedding techniques are commonly used to line characterization and error analysis (network analyzer calibration) [12, 13, 14, 15]. Nevertheless, the explicit determination of scattering parameters of a powder-sample can be obtained in an easier way using the graph method for network branch as graphically presented in Fig. 3, where scattering parameters of the wall are defined as **E**, while scattering matrix of the measured powdered material is presented as **S**.

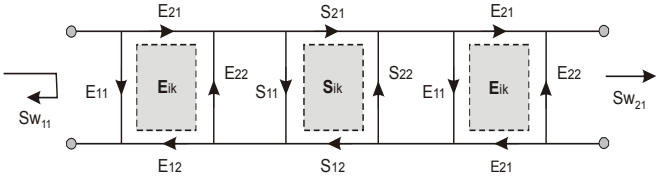

Fig. 3. The graph of the scattering parameters of whole composite - Sw_{ik}, the wall - E_{ik} and powder under test - S_{ik}

For this calculation, the symmetrical and reciprocal properties of these matrices will be taken into account. Using the graph method for network branch one can obtain formulas of resultant scattering parameters **Sw** of the whole composite (material under test and 2 walls) [11]:

$$Sw_{11} = E_{11} + E_{21}\frac{\left(1 - E_{11}S_{11}\right)S_{11} + E_{11}S_{21}^2}{\left(1 - E_{11}S_{11}\right)^2 - E_{11}^2S_{21}^2} \tag{2}$$

$$Sw_{21} = \frac{E_{21}^2 S_{21}}{\left(1 - E_{11}S_{11}\right)^2 - E_{11}^2S_{21}^2} \tag{3}$$

where:
Sw_{ik} – scattering parameters of the whole composite material
E_{ik} – scattering parameters of the wall
S_{ik} – scattering parameters of the powdered sample.

Using formulas (2) and (3) for scattering parameters of a powder-sample the following relationships can be done by:

$$S_{11} = \frac{\left(E_{21}^2 + E_{11}H\right)H - E_{11}Sw_{21}^2}{\left(E_{21}^2 + E_{11}H\right)^2 - \left(E_{11}Sw_{21}\right)^2} \tag{4}$$

978-1-4673-0717-8/12/$31.00 ©2012 IEEE

$$S_{21} = \frac{E_{21}^2 Sw_{21}}{\left(E_{21}^2 + E_{11}H\right)^2 - \left(E_{11}Sw_{21}\right)^2} \quad (5)$$

where:

$$H = Sw_{11} - E_{11}$$

Formulas (4) and (5) allow to calculate the scattering parameters of the powder-sample S_{11} and S_{21} in terms of scattering parameters of the walls E_{11} and E_{21} and parameters of the whole composite Sw_{11} and Sw_{21}. Complex values of E_{ik} and Sw_{ik} have been measured using the vector network analyzer (VNA). Scattering parameters (4) and (5) are the functions of unknown parameters ε and μ of the specimen. Having the scattering parameters of the powder-sample (S_{ik}), it is possible to calculate the permittivity and permeability using the method proposed by Nicolson, Ross and Weir (NRW method) [6, 9]. In their model, values of complex permittivity and permeability are determined according to the following formulas:

$$\mu = -j\frac{1+\rho}{1-\rho}\frac{\lambda}{2\pi d}\ln\left(\frac{1}{T}\right) \quad (6)$$

$$\varepsilon = -\frac{1}{\mu}\left[\frac{\lambda}{2\pi d}\ln\left(\frac{1}{T}\right)\right]^2 \quad (7)$$

where:

$$T = \frac{S_{11} + S_{21} - \rho}{1 - \rho\left(S_{11} + S_{21}\right)} \quad (8)$$

$$\rho = X \pm \sqrt{X^2 - 1} \quad (9)$$

$$X = \frac{1 - V1\ V2}{V1 - V2} \quad (10)$$

$$V1 = S_{21} + S_{11} \qquad V2 = S_{21} - S_{11} \quad (11)$$

and

ρ - reflection coefficient,
γ - propagation constant,
T - transmission coefficient,
λ - wavelength in free space,
d – length (thickness) of the powder-sample.

The above equations allow to determine the complex values of permittivity and permeability of the sample in the coaxial line

IV. Experiments and Results

Material

Amorphous and nanocrystalline powders were measured using the proposed method. Each type of powder – amorphous and nanocrystalline – was sieved to obtain four groups with different particle size. In this study, the following groups of powders were investigated: group A – with particle size smaller than 25 μm, group B – (25 – 50) μm, group C – (50 – 100) μm and group D with particle sizes (100 – 200) μm. After the measurement, the density was determined for each group. For comparison, the bulk density of the investigated metallic glass was of about 7.3 g/cm^3. The powder density for each group has been presented in Table 1.

Table 1. The density of alloy powders.

Group (particle size)	Powder density (g/cm^3)	
	amorphous	nanocrystalline
A (< 25 μm)	3.10 (±0.05)	3.15 (±0.05)
B (25-50) μm	3.30 (±0.05)	3.40 (±0.05)
C (50-100) μm	3.25 (±0.05)	3.15 (±0.05)
D (100-200) μm	2.60 (±0.05)	2.6 (±0.05)

Measurements of permittivity and permeability were performed for four groups of powders with different particle sizes, allowing to see the relationship between amorphous and nanocrystalline structures in function of particle size. Each investigation was done in the frequency range from 0.2 to 10 GHz.

Measurements

Measurements of complex relative permittivity and permeability were carried out using a vector network analyzer. This system consisted of a 7 mm coaxial air-line, equipped with measurement cables and LPC7 connectors. The center conductor of the coaxial air-line is 3.04 mm in diameter to receive the 50 Ω characteristic impedance of the holder. The system measures the magnitudes and phases of S-parameters of a sample. In this case, scattering parameters refer to the composite sample - Sw_{ik}. At first, the empty coaxial air-line was employed to calibrate the system. The additional tools consisted of auxiliary air-lines were used to obtain the calibration. The calibration coefficients were determined by solving a set of simultaneous equations generated from a linear fractional transformation. After calibration, when the system was operated with the errors corrected, the measurements were updated by the calibration coefficients. Data of calibration process and measurements of the sample were acquired using the MultiCal program [10, 16, 17]. The main measurement begins with determination of S-parameters of the wall (E_{ik}) and then the measurement of the composite sample (wall+powder+wall) can be received (Sw_{ik}). This technique of powder measurement with the proposed method was validated using slid state sintered ferrite Ni-Zn instead of powder. The obtained result was within the uncertainty limit, discussed below.

Uncertainty analysis

During measurements of the scattering parameters in coaxial lines, several factors contribute to the uncertainty. Some of these uncertainties are difficult to analyze precisely and can be only estimated. However, it is possible to effectively reduce the above errors taking into account NIST calibration procedures and recommendations [8]. The estimation of the uncertainty in permittivity and permeability measurements are in good agreement with similar observations presented in the literature. The measurement accuracy of ε, μ was about ± 5 %. The obtained data of relative complex permittivity and permeability were presented in Figs. 4, 5, 6 and 7.

978-1-4673-0717-8/12/$31.00 ©2012 IEEE

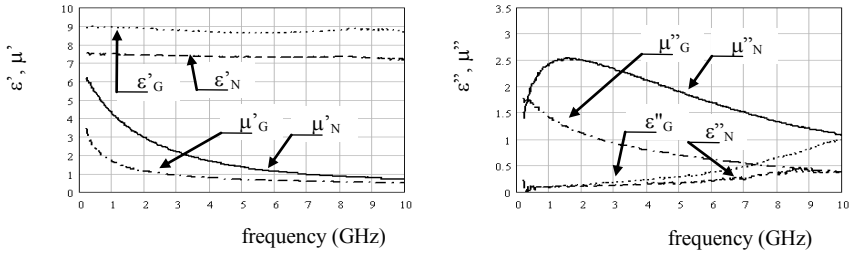

Fig. 4. Relative permittivity and permeability of the amorphous (G) and nanocrystalline (N) powder with particle size < 25 μm (group A)

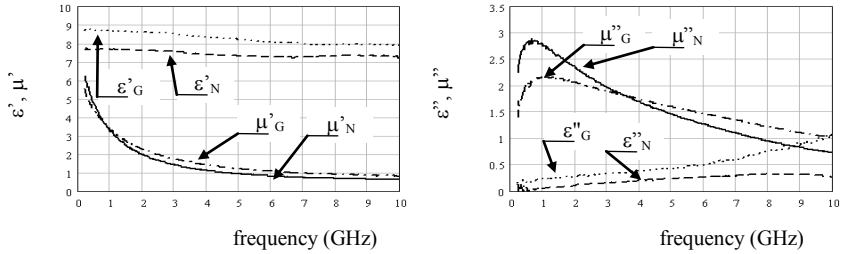

Fig. 5. Relative permittivity and permeability of the amorphous (G) and nanocrystalline (N) powder with particle size of (25-50) μm (group B)

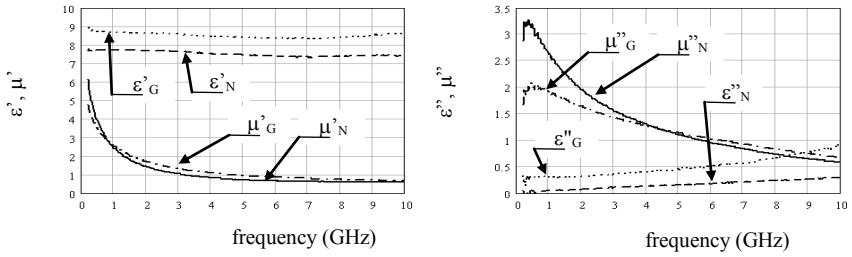

Fig. 6. Relative permittivity and permeability of the amorphous (G) and nanocrystalline (N) powder with particle size of (50-100) μm (group C)

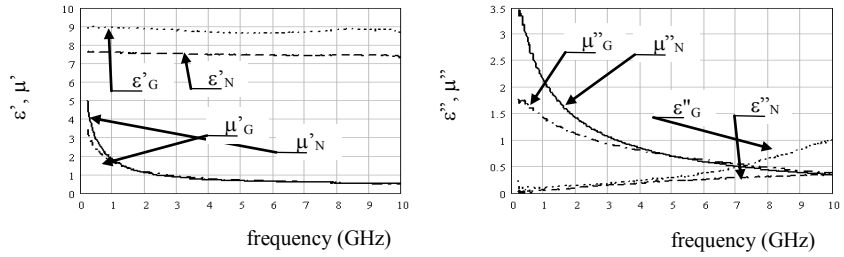

Fig. 7. Relative permittivity and permeability of the amorphous (G) and nanocrystalline (N) powder with particle size of (100-200) μm (group D)

The curves in Figures 4-7 were presented with the following lines:

- for nanocrystalline powder: continuous line – permeability (μ'_N, μ''_N), dashed line – permittivity (ε'_N, ε''_N),
- for amorphous powder: dash-dotted line – permeability (μ'_G, μ''_G), dotted line – permittivity (ε'_G, ε''_G)

Values of permittivity ((ε'_N, ε''_N) and permeability (μ'_N, μ''_N) of nanocrystalline Finemet were presented in our previous work [11] and have been done in common figures for comparison.

The constitutive parameters, presented in Figs. 4-7, are done for pure Finemet powder without any insulating substances. Literature data refers rather to powders immersed into resin, wax, or other glues thus they are relative to the weight or volume relation of the insulating phase used in the measurement. Values of permittivity and permeability of pure pulverized Finemet were not presented.

The figures show that all samples have functions of electric constants markedly flat over the frequency, however the amorphous powders' ε' are significantly higher than these of nanocrystalline ones. Both ε'_G ε'_N of investigated groups do not depend on the particle size. On the other hand, electric loss factors ε''_G ε''_N are monotonically rising with frequency and are quite similar for amorphous and nanocrystalline structure in the lower frequency range, but at higher frequencies amorphous powders have higher values of ε''. Observed differences in ε'' between amorphous and crystalline structure are mainly due to differences in the ionic polarization. Comparing ε''_G and ε''_N of all groups it is easy to see that they are quite similar to each other. From the obtained values one can notice that the electric properties are rather independent from the particle size in the investigated frequency range from 0.2 to 10 GHz.

In the case of magnetic properties the real part of permeability monotonically decreases with frequency. The important observation is that for powders having particle sizes larger than 25 μm (groups B, C and D), the relationships of μ'_G and μ'_N are practically the same. The significant increasing of μ'_N comparing to μ'_G was observed for group A with the smallest particle size.

978-1-4673-0717-8/12/$31.00 ©2012 IEEE

Furthermore, magnetic constants of nanocrystalline powders increase systematically with the decrease of the particle size.

The magnetic loss factor depends on powder structure - amorphous vs. crystalline. For the smallest particles (group A), the magnetic loss factor of nanocrystalline structure is significantly higher than this of an amorphous one over the whole investigated frequency. For groups B, C and D, magnetic loss factors are higher in lower range of the investigated frequencies, while at higher frequencies μ'_G are higher than μ'_N. Magnetic loss factors of nanocrystalline powders reach maxima with the peak positions depending on the particle sizes. The higher value was obtained for the largest particle size (group D), however, this peak is the most narrow in terms of frequency. From the practical point of view, the value of μ''_N for group A is more suitable taking into account the broadband properties of the material and applications for EMC. The presented study is focused on the analysis of pure powder behavior. The final composites made on the basis of nanocrystalline powder bound with dielectrics will have different properties depending on their composition. However, the interpretation of the shielding properties of composites that will be measured in the future, will need to be based on the investigations of pure ferromagnetic powder.

V. CONCLUSION

The aim of this work was to measure the electric and magnetic properties of Finemet alloy with nominal composition $Fe_{73.5}Si_{13.5}B_9Nb_3Cu_1$ and with amorphous and nanocrystalline structure, used as a soft magnetic material, in the frequency range from 0.2 to 10 GHz. The measurements were performed in coaxial lines with an improved calculation technique. The proposed method allows to determine values of permittivity and permeability of powdered magnetic material. Based on this technique, values of relative permittivity (ε', ε'') and permeability (μ', μ'') of the powdered amorphous and nanocrystalline Finemet were obtained for four groups of powders with different particle size.

The obtained results show that the powdered nanocrystalline Finemet consisting of particles below 25 μm in diameter can have good shielding / absorbing properties.

VI. ACKNOWLEDGMENT

This work was carried out with the financial support of the Polish National Center of Research and Development as a research project No OR00006311

REFERENCES

[1] Y. Yoshizawa, S. Oguma, K. Yamauchi, New Fe-based soft magnetic alloys composed of ultrafine grain structure, J. Appl. Phys. 64, v.10, pp. 6044-6046, 1988.

[2] G Herzer, Grain structure and magnetism of nanocrystalline ferromagnets, IEEE Trans. Magn., vol. 25, no 5, 3327-3329, 1989.

[3] F. Mazaleyrat, L.K. Varga, Ferromagnetic nanocomposites, J. Magn. Magn. Mater., 215-216, pp. 253-259, 2000.

[4] M.M. Raja, K.Chattopadhyay, B. Majumdar, A. Narayanasamy, Structure and soft magnetic properties of Finemet alloys, J. Alloys Compd., 297, pp. 199-205, 2000.

[5] M.M. Raja, N. Ponpandian, B. Majumdar, A. Narayanasamy, K. Chattopadhyay, Soft magnetic properties of nanostructured FINEMET alloy powder cores, Mat. Science Eng. A, v. 304-306, pp. 1062-1065, 2001.

[6] W.B. Weir, Automatic measurement of complex dielectric constant and permeability at microwave frequencies, Proc IEEE, vol. 62, pp. 33-36, 1974.

[7] G. Herzer, Grain size dependence of coercivity and permeability in nanocrystalline ferromagnets, Magnetic Conference. 1990 Digests of Intermag' 90. International, 2002.

[8] J. Baker-Jarvis, M.D. Janezic, B.F. Riddle, R.T. Johnj, P. Kabos, C.L. Holloway, C.A. Grosvenor, Measuring the permittivity and permeability of lossy materials: solids, liquids, metals, building materials and negative-index materials, Natl. Inst. Stand. Technol., Technical Note, NIST 2005.

[9] A.M. Nicolson, G.F. Ross, Measurement of the intrinsic properties of materials by time domain techniques, IEEE Trans. Instrum. Meas., vol. 19, pp. 377-382, 1968.

[10] W. Wiatr, R. Frender, M. Żebrowski, Characterization of microwave absorbing materials using a wideband T/R measurement technique, Conference Proceedings on International Conference on Microwaves, Radar and Wireless Communications, Wroclaw, Poland, 2, pp. 475-478, 2008.

[11] R. Kubacki, J. Ferenc, R. Przesmycki, M. Wnuk, The nanocrystalline FeSiBCuNb Finemet absorption properties at microwaves, IEEE Trans on EMC, vol. 54, no.1, pp. 93-100, 2012.

[12] J.L. Carbonero, R. Joly, G. Morin, B. Cabon, On-wafer high-frequency measurement improvements, Proc. IEEE Int. Conference on Microelectronic Test Structures, vol. 7, pp. 168-173, 1994.

[13] G.W. Hanson, J.M. Grimm, D.P. Nyquist, An improved de-embedding technique for the measurement of the complex constitutive paramaters of materials using a stripline field applicator, IEEE Trans. Instrum. Meas., vol. 42, pp. 740-745, 1993.

[14] U.C Hasar, Calibration-independent method for complex permittivity determination of liquid and granular materials, Electronic Letters, vol. 44, no. 9, 2008.

[15] A.M. Mangan, S.P. Voinigescu, M-T. Yang, M. Tazlauanu, De-embedding transmission line measurements for accurate modeling of IC designs, IEEE Trans. Electron Dev., vol. 53, pp. 235-241, 2006.

[16] C.C. Huang, A novel calibration algorithm with unknown Line-Series-Shunt standards for broadband S-parameter measurements, IEEE Trans. Instrum. Meas., vol. 57, no 5, pp. 891-896, 2008.

[17] R.B. Marks, A multiline method of network analyzer calibration, IEEE Trans. Microwave Theory Tech., 42, pp. 1205-1215, 1991.